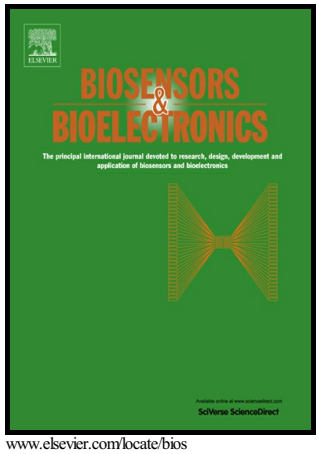

www.elsevier.com/locate/bios

Detection of Vapor-Phase Organophosphate Threats Using Wearable Conformable Integrated Epidermal and Textile Wireless Biosensor Systems

Rupesh K. Mishra, Aida Martín, Tatsuo Nakagawa, Abbas Barfidokht, Xialong Lu, Juliane R. Sempionatto, Kay Mengjia Lyu, Aleksandar Karajic, Mustafa M. Musameh, Ilias L. Kyratzis, Joseph Wang

PII: S0956-5663(17)30711-X
DOI: https://doi.org/10.1016/j.bios.2017.10.044
Reference: BIOS10069

To appear in: *Biosensors and Bioelectronic*

Received date: 22 July 2017
Revised date: 29 September 2017
Accepted date: 18 October 2017

Cite this article as: Rupesh K. Mishra, Aida Martín, Tatsuo Nakagawa, Abbas Barfidokht, Xialong Lu, Juliane R. Sempionatto, Kay Mengjia Lyu, Aleksandar Karajic, Mustafa M. Musameh, Ilias L. Kyratzis and Joseph Wang, Detection of Vapor-Phase Organophosphate Threats Using Wearable Conformable Integrated Epidermal and Textile Wireless Biosensor Systems, *Biosensors and Bioelectronic,* https://doi.org/10.1016/j.bios.2017.10.044

Detection of Vapor-Phase Organophosphate Threats Using Wearable Conformable Integrated Epidermal and Textile Wireless Biosensor Systems

Rupesh K. Mishra, [1,#] Aida Martín, [1,#] Tatsuo Nakagawa,[1] Abbas Barfidokht,[1] Xialong Lu,[1] Juliane R. Sempionatto,[1] Kay Mengjia Lyu,[1] Aleksandar Karajic,[1] Mustafa M. Musameh,[2] Ilias L. Kyratzis[2] and Joseph Wang*[1]

[1]Department of NanoEngineering, University of California, San Diego, La Jolla, California 92093, United States

[2]CSIRO Manufacturing, Clayton, Victoria 3168, Australia

[#] R.K.M, and A.M contributed equally to this work.

*Corresponding Author: E-mail: josephwang@ucsd.edu

Abstract

Flexible epidermal tattoo and textile-based electrochemical biosensors have been developed for vapor-phase detection of organophosphorus (OP) nerve agents. These new wearable sensors, based on stretchable organophosphorus hydrolase (OPH) enzyme electrodes, are coupled with a fully integrated conformal flexible electronic interface that offers rapid and selective square-wave voltammetric detection of OP vapor threats and wireless data transmission to a mobile device. The epidermal tattoo and textile sensors display a good reproducibility (with RSD of 2.5 and 4.2%, respectively), along with good discrimination against potential interferences and linearity over the 90 to 300 mg/L range, with a sensitivity of 10.7 $\mu A \cdot cm^3 \cdot mg^{-1}$ (R^2 0.983) and detection limit of 12 mg/L in terms of OP air density. Stress-enduring inks, used for printing the electrode transducers, ensure resilience against mechanical deformations associated with textile and skin-based on-body sensing operations. Theoretical simulations are used to estimate the OP air density over the sensor surface. These fully integrated wearable wireless tattoo and textile-based nerve-agent vapor biosensor systems offer considerable promise for rapid warning

regarding personal exposure to OP nerve-agent vapors in variety of decentralized security applications.

Keywords: Wearable sensor, Integrated Flexible Electronics, Organophosphate, Nerve agent, Vapor phase detection, OPH-Biosensor

Introduction

The growing global concern over terrorist use of chemical warfare agents (CWA) has motivated extensive research efforts aimed at early detection of such threats. Among these CWA threats, organophosphorus (OP) nerve-agent compounds represent the most disreputable weapons of mass destruction (Kim et al. 2016; Singh 2016). One of the main dangers of such attack are harmful CWA aerosols that create a major vapor cloud that can be transported in the atmosphere over significant distances (Kukkonen et al. 2001; Steiner et al. 2005). In particular, persistent low vapor pressure OP agents, such as Sarin, Soman, or VX, are the most dangerous volatile OP agents and are thus of extreme concern for vapor-phase detection (Steiner et al. 2005; Baker et al. 2014; Yao et al. 2016). Early detection of OP nerve agents is thus extremely important in the defense against terrorist activity. In particular, there are urgent needs for developing rapid, cost-effective on-body (textile- or skin-based) detection strategies for providing rapid warning regarding personal exposure to nerve agents for ensuring an immediate medical treatment. Current CWA detection defense strategies are still relying on conventional lab-based techniques, such as bulky and time-consuming mass spectroscopy-based systems coupled to chromatographic separations, which are not suitable for field settings. The portable instrumentation and low power demands of electrochemical biosensors satisfy many of the requirements of wearable devices and also on-site monitoring of CWA. Enzymatic biosensors, based on OPH, have thus received a considerable recent attention toward decentralized measurements of OP threats in liquid (Mulchandani, et al, 1999; Singh 2016; Zhang et al. 2014) and dry (Mishra et al., 2017a) phases, but have not been applied for vapor-phase detection using wearable platforms.

Wearable sensors technology offers considerable promise to address these growing defense and security needs. While wearable chemical sensors have experienced significant progress over the past 5 years (Bandodkar et al. 2014; Gao et al. 2016; Kim et al. 2015; Bandodkar et al. 2015a; Bandodkar et al. 2016), the majority of the new on-body skin and textile-based chemical sensing devices have focused on healthcare and fitness monitoring of selected biomarkers. Several wearable devices, based on textiles, gloves, microneedles, or air balloons have been introduced recently for variety of defense applications (Cánovas et al. 2016; Chuang et al. 2010; Mishra et al. 2017a; Mishra et al. 2017b; Zhu et. al 2016), but not in connection to real-time monitoring of vapor-phase OP agents. Zhu et al described recently a single-use dosimetric badge for detecting the hazardous agent diethylchlorophosphate (Zhu et al, 2016).

The present work demonstrates the first example of a wearable OPH-based skin and textile-worn biosensors for continuous vapor-phase detection of OP threats (**Figure 1**). The skin-mounted flower-like tattoo (**Figure 1B**) and textile-based (**Figure 1C**) electrochemical biosensors have been fabricated with elastomeric inks and display resiliency toward mechanical stress expected from the wearer's activity without compromising the biosensing performance. The electrochemical detection is carried out using a soft, flexible electronic board integrated with the epidermal and textile sensors (see **Figure 1D** and **1E**). The new electronic interface (on a polyimide-based substrate) maintains its functionality under mechanical stress and retains conformal contact with the skin. It contains the potentiostatic circuitry and waveform generator for executing rapid square-wave voltammetry (SWV) detection of the enzymatically-generated nitrophenol product. The coupling of the specific OPH enzymatic reaction with the potential-scanning SWV transduction offers a dual dimension of selectivity towards the target OP threat. A simple mesh nebulizer has been used for the OP vapor generation with theoretical modelling simulates the resulting vapor OP profile. As illustrated in **Figure 1A** and **Video S1**, OP vapors, in the form of micro-droplets, are released by the nebulizer onto the skin-based sensor, worn on a mannequin's arm for safety reasons (Experiments were conducted in double layered glove box within a fume hood, described in the Experimental section). The electrode transducer surface is coated with a conducting gelatin gel layer which allows diffusion of the target OP vapors. The voltammetric data are transmitted wirelessly to a mobile device using Bluetooth communication.

The attractive design and performance characteristics of the new wearable OP vapor biosensor system hold considerable promise for rapid on-body detection and warning of CWA threats towards a timely countermeasure action and the protection of soldiers and civilians. Our current effort aims at addressing the growing demands of alerting and protecting soldiers and civilians against possible direct exposure to vapor-phase organophosphate threats from their surrounding environment. Placing OP biosensors on the textiles or skin body barriers would thus provide the ultimate warning against such personal exposure. The skin-based sensing is particularly crucial for triggering instantaneous countermeasure for OP skin exposure towards a timely autonomous therapeutic intervention. Besides defense applications, the new wearable sensor offers great promise for protecting farmers from direct exposure to pesticides. Such on-body detection, rapid warning and timely decontamination are expected to dramatically change the protection of our civilians, farmers, and military personnel.

Experimental Section

Chemical and reagents

Potassium ferricyanide, dipotassium hydrogen phosphate (K_2HPO_4), potassium dihydrogen phosphate (KH_2PO_4), gelatin (from porcine skin, Type A), sodium acetate, methyl paraoxon, polystyrene-block-poly-isoprene-block-polystyrene (PS-PI-PS) (styrene 14 wt.%), ferricyanide sodium hydroxide, acetone, Nafion® and ethanol were purchased from Sigma Aldrich (USA). All chemicals were of analytical grade and were used without further purification. Ultra-pure deionized water was used in the preparation of the aqueous electrolyte. The OPH enzyme (10 µg/mL), provided by CSIRO (Australia), was isolated from *E. coli* bacterial strain DH5α. The isolation, expression, purification and crystallization were performed by the procedure described by Yang et al.(Yang et al. 2003). The Inkjet temporary tattoo paper was acquired from Papilio™ (Rhome, TX, USA). The experimental details of ink formulation, electrode fabrication, hydrogel preparation, enzyme immobilization, mechanical resiliency tests and designing/fabrication of electronic board is described in the electronic supplementary material.

Vapor phase detection of OP nerve agent through Nebulizer

Due to the toxicity of OPs, practical defense scenarios were mimicked in the lab conditions using a double-layer glove box (within a fume hood) by placing the sensor on a mannequin arm. A portable compact Mesh Nebulizer (mini Air 360+A, LFS, Shenzhen, China) was used during all experiments under safe conditions. To ensure such safety, the experimental set-up consisted in a sealed bag-based glove box (4 gal capacity), containing an airtight (1 gal capacity) polymer box inside. This rigid box had a circular hole to insert the Nebulizer inlet. The complete set up was placed inside the fume hood with continuous air flow. The bag-based glove box was double layered protected with an additional bag-based glove box to provide further protection from the OP vapors nebulized inside the fume hood. Prior to sealing the double-layered glove box, the epidermal tattoo or textile-printed biosensor was transferred or attached on a mannequin, respectively. Subsequently, the flexible soft electronic board was connected below the electrodes. Both connections and electronic board were isolated using transparent film adhesive (3M, US). The mannequin was then placed inside the airtight polymer box along with Mesh Nebulizer (containing OP solution). The data was wirelessly monitored with a smart-device (laptop) via Bluetooth network. Various concentrations (0, 5, 10 and 15 mM) of MPOx solutions were prepared in DI water and used through the nebulizer to mimic realistic settings in the lab conditions. The nebulizer sprayed the MPOx onto the sensor surface for different times (ranging from 15 to 45 s), and the electrochemical response was recorded using the integrated flexible board by square-wave voltammetry over the +0.3 to +1.2 V range, using a 10 Hz frequency and amplitude of 25 mV. The enzymatically generated *p*-nitrophenol product upon spraying the OP vapor on sensor surface, was oxidized and detected voltammetrically based on its anodic peak at +0.85 V. Similar experiments were carried out using the printed textile sensor. The response of both the skin-worn and textile biosensors was recorded with the flexible wireless conformal electronic board. The disposable biosensors were used one-time to avoid carry-over and false alarms due to accumulation of the OP targets on the gel between experiments.

Safety Note: Due to the extreme toxicity of OP compounds and their use in terrorist activities, the realistic scenarios were mimicked in lab conditions using a double layered glove box inside the fume hood. An airtight polymer box was placed inside the glove box to position a mannequin

arm and subsequently the tattoo or textile sensor was placed on to the center of the arm. Experiments were conducted by following complete safety measures, wearing safety goggles and respiratory mask.

Results and Discussions

Design of epidermal tattoo and textile sensor with soft electronics

The wearable epidermal tattoo and textile-based biosensors were fabricated using screen-printing technology. **Figure 1A** shows an image of the OPH-based wearable sensing platform that integrates the stress-enduring flower-like printed electrode system and the flexible electronic interface, along with the corresponding equations for the enzymatic and detection reactions. Vapor of the nerve-agent threat is generated at room temperature exploiting a nebulizer, which produces ~2 μm aqueous microdroplets of the target OP. A conductive semi-solid gelatin gel on the sensing area of the working electrode facilitates completion of the electrochemical cell. The OP (*i.e.*, methyl paraoxon (MPOx)) hydrolysis product, *p*-nitrophenol, is subsequently oxidized on the working electrode during an anodic SWV scan to yield an anodic peak current proportional to the target OP.

The wearable electrochemical biosensor is relied on elastic conducting inks printed on the tattoo paper, and transferred onto the skin, as illustrated in **Video S2**. First, a silver layer, based on Ag/AgCl ink combined with the Ecoflex elastomer, is used for printing the reference electrode. Subsequently, a second stretchable layer consisting of a carbon ink modified with PS-PI-PS elastomer is used for printing the working and counter electrodes, imparting resilience against mechanical strains. Such resilience against mechanical deformations is illustrated in the images of both the epidermal tattoo sensor (**Figure 1B**) and textile sensor on a lab coat (**Figure 1C**). These wearable biosensors offer rapid and on-site voltammetric detection of nerve-agent threats via SWV monitoring of the enzymatically-generated *p*-nitrophenol. Such voltammetric operation is controlled by a wearable and flexible electronic board, as shown in **Figure 1D** and **1E**, for the

skin tattoo and textile printed biosensors, respectively. The corresponding voltammograms are transmitted wirelessly to a mobile device (i.e. phone or laptop) via a Bluetooth communication.

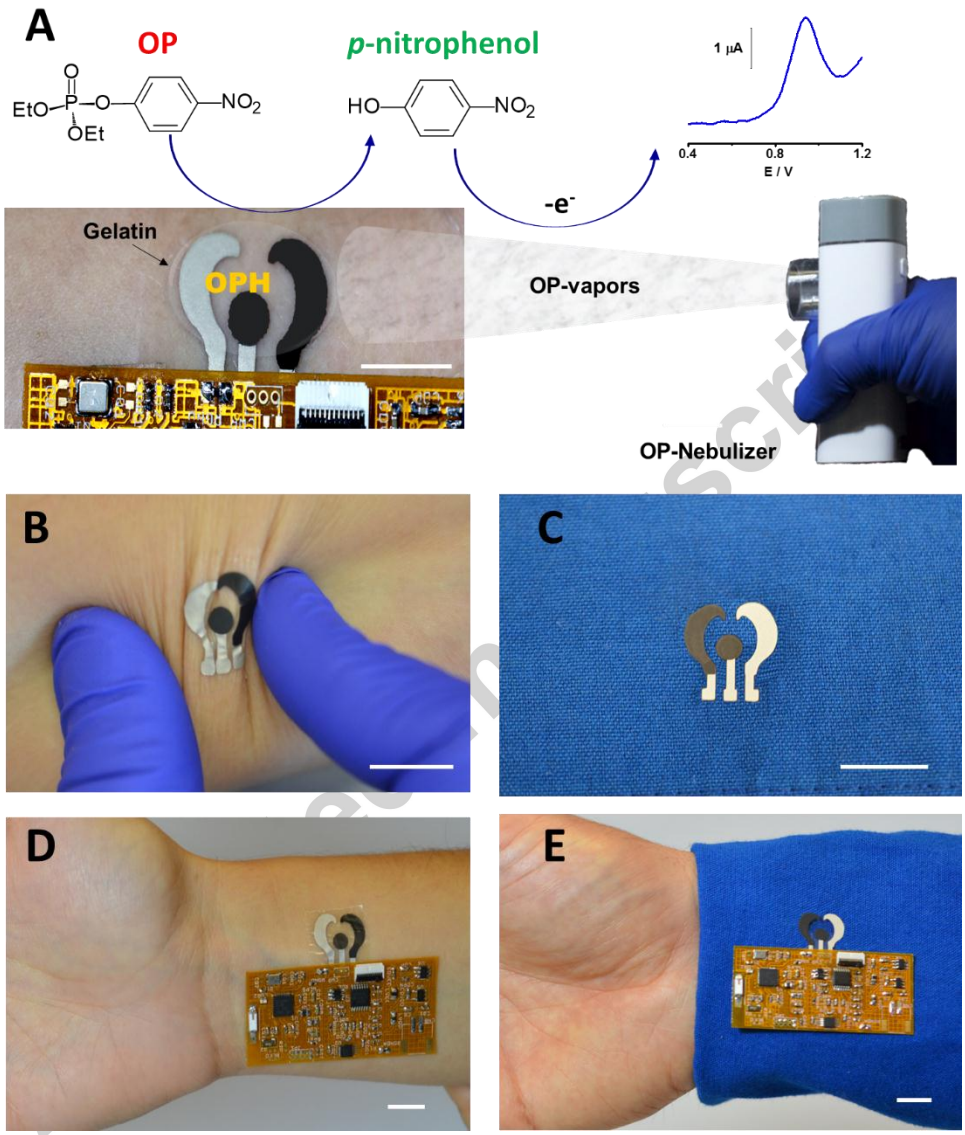

Figure 1. *Flexible skin- and textile-based biosensors for vapor-phase detection of OP agents.* ***(A)*** *Schematic of the experimental set-up of the epidermal tattoo biosensor consisting in flower-like three-electrode system with the OPH-modified working electrode and casted with conductive gelatin gel, connected to the skin-conforming electronic board, along with the nebulizer used for continuous vapor generation during the measurement. OP (MPOx) micro-droplets released from the nebulizer (right) interact with the OPH layer to yield p-nitrophenol product, which is detected using SWV.* ***(B)*** *Deformation of the skin-worn tattoo biosensor; (C) textile-printed biosensor. Photographs of the fully integrated flexible wireless biosensor system on the skin (D)*

and textile (blue lab-coat) (D). The voltammetric results are transmitted wirelessly for rapid alert and display on a laptop device; scale bars, 10 mm.

Electronic circuit design for printed wearable sensors

The biosensor has been connected to a flexible conformal lab-designed wearable wireless and small potentiostat. The electronic PCB, shown in **Figure 2A,** was developed on a polyimide substrate, which was mounted onto the skin to provide the required mechanical flexibility and resilience to potentiostatic circuitry. To the best of our knowledge, this 50 x 24 mm board is the smallest wireless flexible potentiostatic board reported capable of recording SWV measurements. The board contains a SWV circuit **(c)** designed for three-electrode system: working (WE), counter (CE) and reference (RE) electrodes (**Figure 2B**). The SWV circuit is capable of applying scanning potential SWV excitation waveform, and is being controlled by a micro controller unit (MCU) **(b)**. The MCU integrates an analog to digital converter (ADC) for measuring the current at WE, and a Bluetooth Low Energy (BLE), which is connected to a small chip antenna **(a)**, for wireless communication with the BLE host device **(d)** connected to a laptop (or another mobile device). As illustrated in **Figure 2C**, this flexible electronic interface (on the polyimide substrate) can endure severe mechanical strains expected during on-body operation, e.g., bending displayed in this figure to offer conformal skin contact and device functionality under stress.

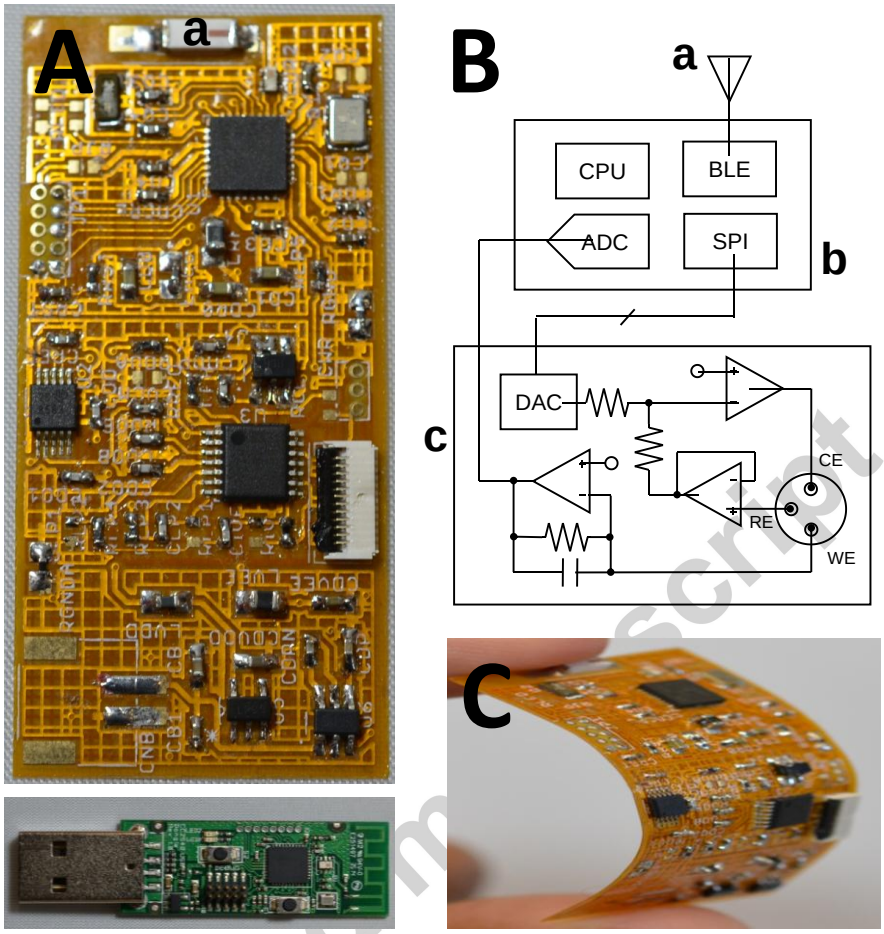

Figure 2*. Flexible electronic backbone for control of the square-wave voltammetric detection and related wireless signal transmission.* ***(A)*** *Original photograph and* ***(B)*** *block diagram of soft flexible electronic PCB show in its components:* ***(a)*** *antenna,* ***(b)*** *microcontroller,* ***(c)*** *SWV circuit,* ***(d)*** *BLE host device; see experimental section for details.* ***(C)*** *Image of the bended flexible electronic board under stress.*

Vapor phase detection and air density determination of nerve agent

In this work, we demonstrated a wearable flexible epidermal tattoo and textile OPH biosensors integrated with a soft conformal electronic circuit board for selective screening of OP nerve agents, in the presence of various other vapor-phase constituents. The soft electronic circuit board was designed to perform the detection of the OP vapor threats through SWV measurement of the *p*-nitrophenol product of the OPH reaction over scanned potential range (+0.3 to +1.2 V).

The flexible electronic interface thus performs the signal transduction, processing and transmission while mounted onto the skin or textile surface.

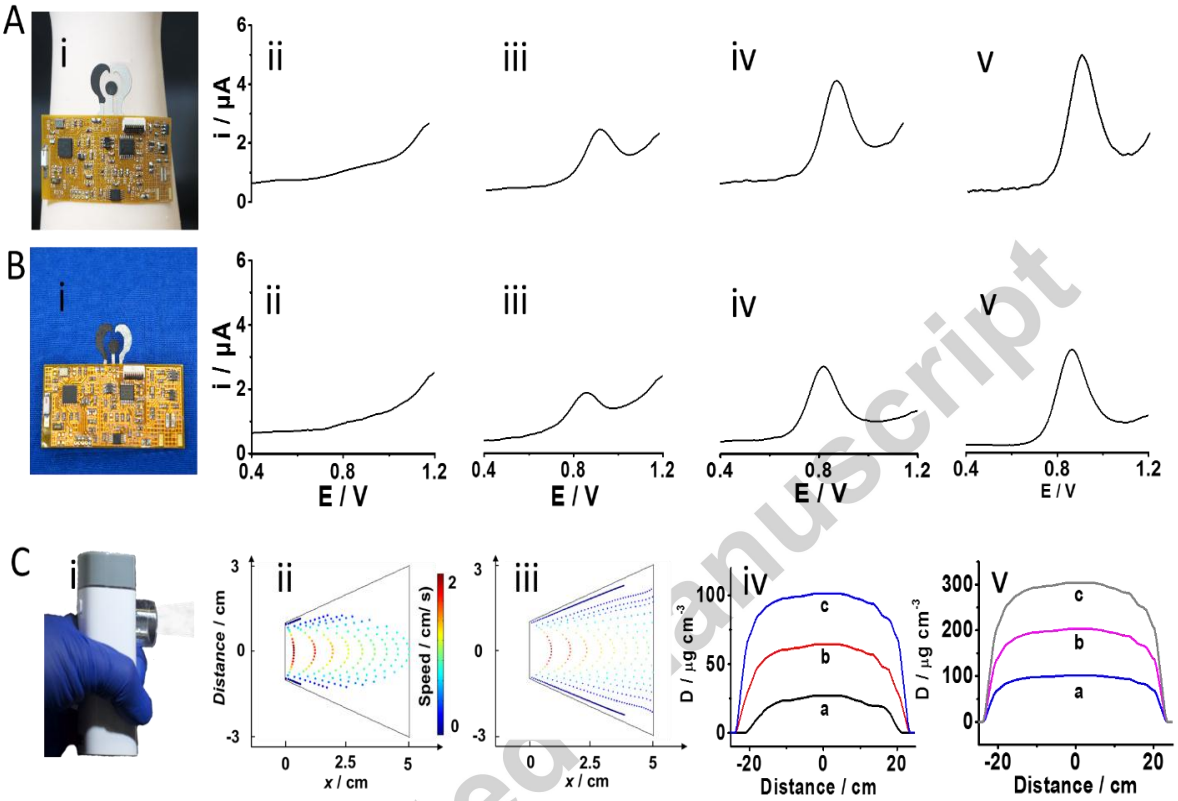

Figure 3: *Vapor-phase detection of MPOx for screening of OP nerve agent using OPH based epidermal tattoo (A) and textile (B) based biosensors. (i) Original images of biosensor integrated with the flexible electronic interface. SWV response upon spraying (ii) 0, (iii) 5, (iv) 10 and (v) 15 mM MPOx in the vapor phase. (See experimental section for details). (C) (i) Image of the OP-spraying nebulizer; (ii) Time lapse image of simulated OP particle trajectories at 4.2 s and (iii) at 45 s spraying time from the nebulizer inlet (left boundary) to the electrode (right boundary), obtained from Video S3 (iv) Theoretical OP density of micro-droplets on the electrode surface using 5 mM OP and different spraying times: 15 (a), 30 (b) and 45 s (c); and (v) theoretical droplet density for different OP concentrations: 5 (a), 10 (b) and 15 mM (c) after a 45 s spraying time. (See experimental section for details).*

The OP vapors were generated by using a mesh nebulizer spray. Due to the toxicity of OP compounds and their use in terrorist activities, we mimicked realistic defense scenarios on a

mannequin arm, as shown in **Figure 4A**. Subsequently, a tattoo or textile sensors were placed on to the center of the arm (**Figure 3Ai and Figure 3Bi)**. As illustrated in **Figure 3**, different MPOx concentrations, ranging from 5 to 15 mM (each 5 mM increment), were used to generate vapor and their voltammetric response was recorded by SWV using integrated flexible board. Different nebulizer spraying times (15 s, 30 s and 45 s) were examine at 5 cm distance from the sensor surface (**Figure S1A**). The 45 s spraying time was found to be the most suitable for further experiments, as it yielded the maximum current value and a distinct peak. Following the selection of the spraying time, we optimized the distance from the vapor source to the working electrode. The vapor phase OP was thus released by the nebulizer from different distances (5, 7.5 and 10 cm) between the inlet source and the sensor surface, with the 5 cm distance offering the best response (**Figure S1B)**. The low signals at larger distances reflects the microdroplet coalescence, the low spray power intensity and the vapor diffusion through the gelatin that decrease the probability of OP vapors to reach to the electrode surface. The performance of the epidermal tattoo and textile sensors was monitored separately in vapor phase. **Figure 3A (ii-v)** and **3B (ii-v)** illustrates the resulting response of OP vapor detection upon spraying on both epidermal tattoo and textile sensors, respectively. As illustrated, a sharp well-defined SWVs response, characteristic of *p*-nitrophenol oxidation peak, is observed at +0.85 V (vs Ag/AgCl), indicating the positive detection of MPOx vapors. On the contrary, not detectable signal is observed in the absence of MPOx vapors (**Figure 3A, ii and 3B, ii**). It is significant to note that the epidermal tattoo and textile sensor is designed for a single-use, since OP vapors are accumulated on the gelatin gel surface and their re-usability might result in false positive; single-use sensor operation eliminates this potential cross contamination. Under humid chamber storage, the fully-modified electrodes can be used up to four days with an optimal analytical performance (RSD< 5% (n=3). In addition, the OPH/Nafion-modified transducer (without agarose overlayer) retains good storage stability up to 7 days when kept in the refrigerator (4ºC) with a RSD of 5.5% (n=7). The new developed wearable and flexible biosensor is also capable of distinguishing between OP vapors based on different MPOx levels, from 5, 10 to 15 mM. The OP vapor sensor showed linearity (R^2 0.983) over the 2.5 mM - 15 mM range, with a sensitivity of 0.3420 µA/mM and a detection limit of 2.5 mM.

The corresponding SWV current signals increase linearly with the concentration. The sensor reproducibility of the developed textile and tattoo biosensor was also examined for vapor -phase

detection of nerve agents. Three different sensors were tested upon the spraying of 5 mM MPOx vapor. The resulting voltammograms for epidermal tattoo and textile, displayed in **Figure S2A** and **S2B,** illustrates good sensor reproducibility with RSD values of 2.5 and 4.2%, respectively. These values confirm the good inter-electrode reproducibility, uniform ink composition and electrode fabrication, and precise design and integration of epidermal and textile sensor with soft electronic board. Other factors that may affect the sensor reproducibility include gel preparation, spraying pattern, accumulation and interaction of OP vapors with the OPH enzyme. These parameters have minimal effect on the response and the screening goal of the new wearable OPH sensor.

Furthermore, the OP vapor density was calculated in the nebulization area. For that, we theoretically simulated the OP droplet distribution by COMSOL, considering an OP vapor source of 2 cm (left boundary) as the inlet of the nebulizer, and the working electrode area (in the middle of the right boundary) at 5 cm distance. A two dimensional model considering 2 μm OP microdroplets propelled by an air flow of 0.9 mL/min was simulated, as shown in **Video S3**. Using the particle tracing for fluid flow interface model allows to calculate the liquid droplet motion trajectories induced by the air flow. **Figure 3C, ii, iii** show the time-lapse images for the simulated OP microdroplet trajectories and its corresponding speed at the studied area. It is noticeable that the highest speed around 2 $cm \cdot s^{-1}$ is shown, as expected, in the area close to the OP vapor source. It was also estimated that in the initial 4.2 s, OP microdroplets started to reach the working electrode. After 45 s, (**Figure 3C, iii**) all the OP microdroplets occupy a larger electrode area. The number of OP droplets passing through the electrode (right boundary) can be theoretically estimated based on the different concentrations of OPs being tested and spraying time. **Figure 3C, iv** and **3C, v** shows the OP density distribution on the electrode surface, considering the center of the working electrode as distance 0 at different conditions. As illustrated in the **Figure 3C, iv**, the OP density distribution was estimated for 5 mM OP at different spraying time intervals (15s, 30 s and 45s). Subsequently, after selecting the optimal (45 s) spraying time, we estimated the OP density distribution for different OP concentrations (5, 10 and 15 mM). As expected, the OP density distribution increases with the spraying time and concentration. For instance, OP densities in the center of the sensor varies from 25 $\mu g \cdot cm^{-3}$ (15 s) to 100 $\mu g \cdot cm^{-3}$ (45 s). A similar behavior is observed with increment of the OP concentrations

from 100 $\mu g \cdot cm^{-3}$ (5 mM OP) to 300 $\mu g \cdot cm^{-3}$ (15 mM). Although, this is an accurate approximation, but these theoretical values should be taken as a theoretical overestimation of the experimental OP density. This theoretical model does not consider other (i.e. gravitational, friction, etc.) forces, which may affect the distribution profile of microdroplets and consequently the OP density. Theoretical simulations which allowed to calculate the OP density in a controlled environment of air are also a valuable tool to foreseeing possible hazards. The OP sensor showed linearity (R^2 =0.983) over the 90 - 300 mg/L range, with a sensitivity of 10.7 $\mu A \cdot cm^3 \cdot mg^{-1}$ in terms of OP air density. The cut-off OP value detected by the skin-worn wearable sensors is 2.5 mM that corresponds to an air density 12 mg/L. The tested sensors thus represent a rapid screening tool in close contaminated environment against OP chemical threat.

Selectivity of the wearable sensor

The presence of other co-existing chemical vapors in the environment may influence the selectivity and hence the accuracy of the wearable OP vapor sensor. Accordingly, a selectivity study was conducted using different potential interferences. The results, shown in the **Figure 4B–4I,** indicate that the presence of several common non-target vapors in the environment does not interfere during the on-body OP detection. Note that these seven vapors do not display any anodic (oxidation) SWV signal or affect the corresponding background current.

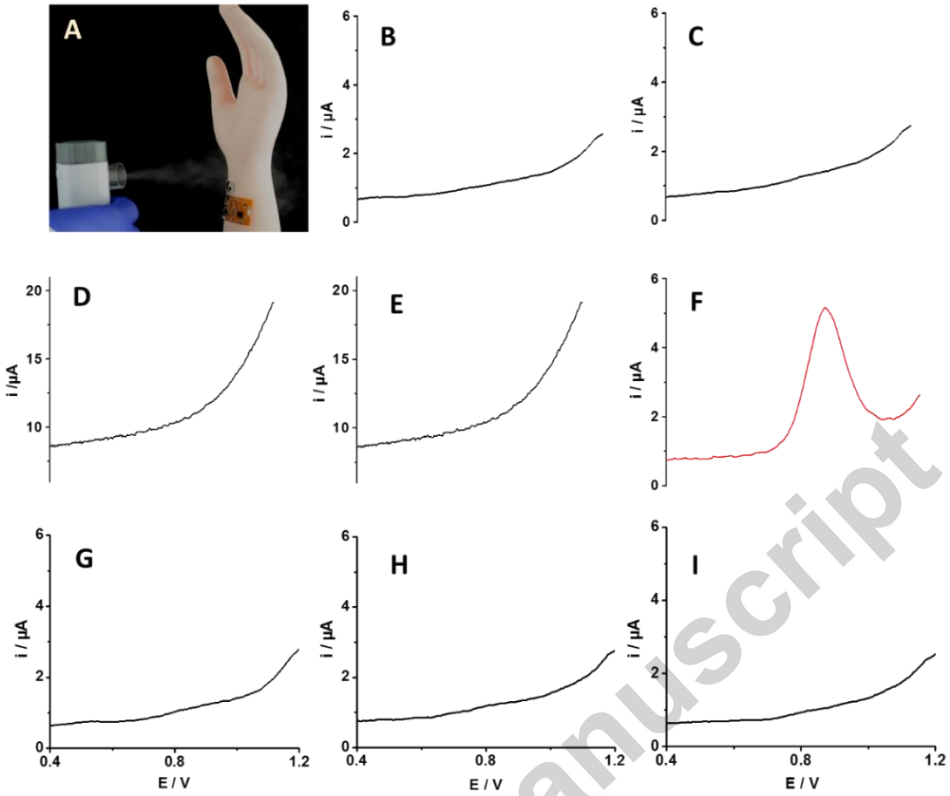

Figure 4. *Selectivity of the epidermal OPH biosensor towards the target OP vapors. (A) Original picture of nebulization (spray) onto the mannequin arm. SWV response of (B) formaldehyde, (C) acetone, (D) 90% methanol, (E) 70% ethanol, (F) 15 mM MPOx, (G) 1 ppm DNT (in 0.5 M NaCl), (H) 70% isopropyl alcohol, (I) 0.1 M PBS/0.1 M KCl. Spray time 45 s. (See experimental section for more details).*

The selectivity of the epidermal tattoo (shown in **Figure 4A**) and textile sensor was evaluated for OP vapor detection in comparison to other common, potentially co-existing vapors. These control vapors were selected based on their presence in the natural environment (Hu et al. 2010; Sylvia et al. 2000; Wei et al. 2006). **Figure 4(B–I)** illustrates the high selectivity of the system for the anodic scan comparing the voltammetric signals of possible interfering vapors with that of an OP target. These data show no anodic signals over the 0.4 to 1.2V range in the absence of OP residues. These control voltammograms correspond to formaldehyde, 90% methanol, 70% ethanol, and acetone vapors (**Figure 4B, C, D** and **E,** respectively). Similarly, a featureless baseline and no signal is observed in **Figure 4 G, H** and **I** for SWV of 1 ppm dinitrotoluene (DNT), 70% isopropyl alcohol (IPA) and buffer, respectively. In contrast, as illustrated in **Figure**

4F, a defined, sharp anodic peak of *p*-nitrophenol oxidation is observed in the presence of the OP target vapor (15 mM MPOx). These selectivity tests strongly support that the observed voltammetric response is due to the presence of MPOx and not due to the other interferences. Such performance reflects the dual dimension of selectivity associated with the coupling of specific OPH enzymatic reaction and potential-scanning voltammetric detection. Overall, the data of **Figure 4** support the potential of the new epidermal biosensor towards the vapor-phase detection of OPs in warfare scenarios. Similarly, control experiments were also conducted to examine the response of the OPH-free transducer towards OP vapors **(Figure S2C).** As expected, no SWV anodic response is observed for 5 mM MPOx in the absence of the enzyme, reflecting the crucial role of OPH enzyme for OP vapor screening.

Mechanical deformation studies

Stress-enduring inks to provide natural and compatible elasticity between the device and the skin, and resilience to the biosensor structure were adopted to screen-print the sensor structures due to its promising features. To examine these features, different mechanical deformation tests were carried out on the skin and textile. First, the epidermal OP-tattoo sensor was subjected to multiple stress deformations while adhering to skin. As shown in **Figure 5**, the stress deformation tests consisted of severe pinching (**Figure 5A**) and twisting (**Figure 5B**). The tattoo sensor maintained its structural integrity and withstand these multiple mechanical deformations while maintaining their attachment to the skin (**Figure S3A)**. Next, the electrochemical properties of the printed textile sensors were investigated using cyclic voltammetry (CV) of the 1 mM ferricyanide redox probe. **Figure 5C** shows the electrochemical performance of textile-based sensor after 100 iterative bending. The experiments were carried out by complete bending of the working and reference electrodes (as shown in **Figure 5F** and **Figure S3B**) and relaxation to the initial position. No significant differences are noticed in the CV of textile sensor performance before (black plot) and after (red plot) the mechanical deformation. Bending studies were also performed in the presence and absence of gelatin conductive gel on the textile sensor surface.

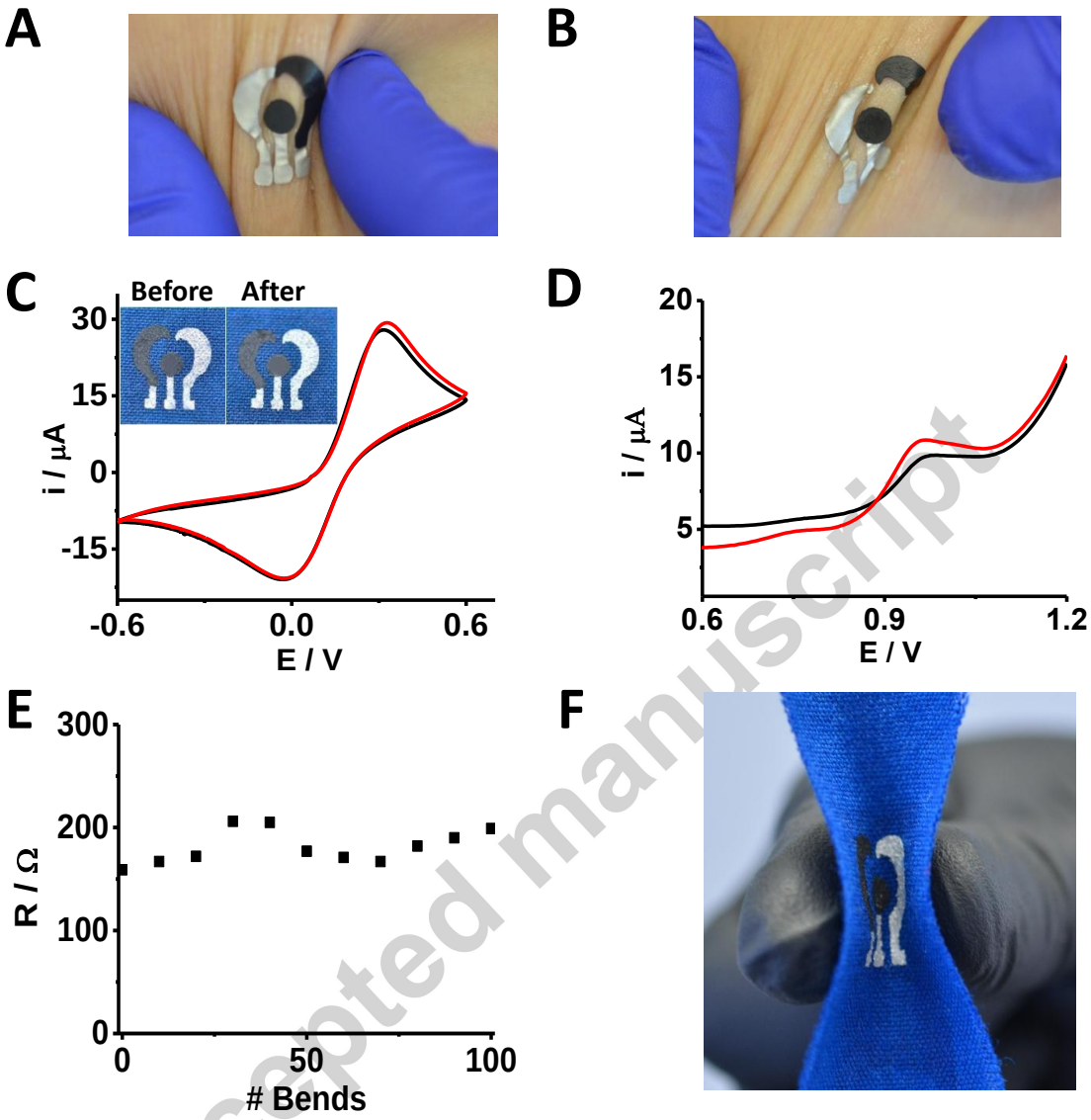

Figure 5. *Visual examination of epidermal-tattoo resiliency after* ***(A)*** *pinching,* ***(B)*** *twisting. Influence of extreme bending stress on the OP-textile based biosensor. Scale 10 mm.* ***(C)*** *Cyclic voltammetry of 1mM ferricyanide (in 0.1 M KCl) recorded before (black plot) and after (red plot) applying 100 iterative bending, as shown in the inset. Scale 5 mm.* ***(D)*** *SWV response of OP vapors before (red curve) and after (black curve) the 100 consecutive bending of the textile sensors.* ***(E)*** *Resistance data points for 100 iterative deformations of the textile-based electrode in the relaxed position.* ***(F)*** *Image showing the bending of the textile sensor at 180 ºC after applying 100 iterative* bending. Scale 10 mm.

As displayed in the **Figure 5D**, even after the 100 iterative bending in the presence of conductive gelatin gel, the textile sensor is still functional and detects OPs without significant changes in the

current response. This clearly shows the effectiveness, usefulness and applicability of the developed sensor to potential field settings. Furthermore, dynamic resistance measurements were also performed to evaluate the influence of bending deformation. As shown in **Figure 5E,** continuous bending cycles of the textile based biosensor were performed up to 100 iterations. The sensor displayed a negligible change of the electrode resistance, with an average resistance value of 181 ± 17 Ω for the first 100 bending. Such behavior indicates that mechanical deformation of the OP-vapor biosensor does not compromise its electrical properties. Upon repeated bend/relax cycling of the fabric using 30 s interval time between positions and cycling, the resistance between the carbon-based working electrode to the end of the silver contact pad was measured, as presented in **Figure S3C** and **S3D**. The resistance values indicated the stability of the electrode with values around 157±12 Ω and 52±9 Ω at relaxed and bended positions, respectively. Such low resistance changes reflect the remarkable resilient to mechanical deformations associated with the stress-enduring ink formulations used for sensor printing.

Conclusions

The monitoring of OP vapors in the warfare environments is of utmost importance during warfare and terrorist activities. Towards this direction, we reported here on the first example of a wearable OPH-based skin- and textile-worn biosensors for continuous vapor-phase detection of OP threats. The new wearable OPH biosensors intimately merge and integrate a skin-conforming epidermal tattoo and textile-based stress-enduring printed electrodes with a soft, flexible, skin-conforming electronic interface. The resulting on-body wearable sensor platform responds instantaneously to exposure to OP vapor and transmits its analytical data wirelessly data to a mobile device that alerts the wearer of such chemical threat. High selectivity is achieved by coupling the specific enzymatic reaction with potential scanning SWV detection. Remarkable resiliency against mechanical deformations was achieved by using strain-persistent printable electrode patterns and conformal electronic interface to offer smooth mounting on the skin and integration with textiles. The attractive performance and design characteristics of the new conformal OP biosensor system provides a rapid warning regarding personal exposure to CWA threats. Theoretical simulations have been used for calculating OP air density distribution. Such real-time data would enable the rapid screening of OP agents for protecting soldiers and

civilians. We envision that the new wearable biosensing platform can be extended or reconfigured for real-time detection of different CWA threats and hazardous vapors to offer a rapid alert in variety of practical defense settings and scenarios. While the MPOx pesticide has been used (for safety reasons) as a model OP nerve-agent, the wearable biosensor concept could be expanded to other nerve agents in connection to immobilized enzymes generating other detectable products (e.g., fluoride ions upon cleaving the P-F bond of sarin or soman). Besides defense applications, the present OPH-based wearable sensor system, involving voltammetric detection of the nitrophenol product, offers promise for protecting agricultural workers and people living near farms from direct exposure to pesticides. The new epidermal sensor system could open the door to a close-loop monitoring-decontamination system for protecting our soldiers, civilians, and farmers via an effective and timely countermeasures upon detection of skin exposure. For both applications, the new wearable sensor could open the door to a close-loop monitoring-decontamination system towards effective countermeasures for protecting our soldiers, farmers and civilians.

Acknowledgments

This work was supported by the Defense Threat Reduction Agency Joint Science and Technology Office for Chemical and Biological Defense (HDTRA 1-16-1-0013). The authors thank Dr. Yuan Gao and Dr. Colin Scott (CSIRO) for their help in purifying the OpdA enzyme.

References

Baker, P.A., Goltz, M.N., Schrand, A.M., Kim, D.-S., 2014. Organophosphate vapor detection on gold electrodes using peptide nanotubes. Biosensors and Bioelectronics 61, 119-123.

Bandodkar, A.J., Jia, W., Yardımcı, C., Wang, X., Ramirez, J., Wang, J., 2014. Tattoo-based noninvasive glucose monitoring: a proof-of-concept study. Anal. Chem. 87, 394-398.

Bandodkar, A.J., Jia, W., Wang, J., 2015. Tattoo-Based Wearable Electrochemical Devices: A Review. Electroanalysis. 27, 562–572.

Bandodkar, A.J., Jeerapan, I., Wang, J., 2016. Wearable chemical sensors: Present challenges and future prospects. ACS Sensors 1, 464-482.

Cánovas, R., Parrilla, M., Mercier, P., Andrade, F.J., Wang, J., 2016. Balloon Embedded Sensors Withstanding Extreme Multiaxial Stretching and Global Bending Mechanical Stress: Towards Environmental and Security Monitoring. Advanced Materials Technologies Adv. Mater. Technol., 1, 1600061.

Chuang, M.C., Windmiller, J.R., Santhosh, P., Ramírez, G.V., Galik, M., Chou, T.Y., Wang, J., 2010. Textile based electrochemical sensing: effect of fabric substrate and detection of nitroaromatic explosives. Electroanalysis 22, 2511-2518.

Gao, W., Emaminejad, S., Nyein, H.Y.Y., Challa, S., Chen, K., Peck, A., Fahad, H.M., Ota, H., Shiraki, H., Kiriya, D., 2016. Fully integrated wearable sensor arrays for multiplexed in situ perspiration analysis. Nature 529, 509-514.

Hu, P., Du, G., Zhou, W., Cui, J., Lin, J., Liu, H., Liu, D., Wang, J., Chen, S., 2010. Enhancement of ethanol vapor sensing of TiO_2 nanobelts by surface engineering. ACS applied materials & interfaces 2, 3263-3269.

Kim, J., de Araujo, W.R., Samek, I.A., Bandodkar, A.J., Jia, W., Brunetti, B., Paixão, T.R., Wang, J., 2015. Wearable temporary tattoo sensor for real-time trace metal monitoring in human sweat. Electrochemistry Communications 51, 41-45.

Kim, T.-I., Maity, S.B., Bouffard, J., Kim, Y., 2016. Molecular Rotors for the Detection of Chemical Warfare Agent Simulants. Analytical Chemistry 88, 9259-9263.

Kukkonen, J., Riikonen, K., Nikmo, J., Jäppinen, A., Nieminen, K., 2001. Modelling aerosol processes related to the atmospheric dispersion of sarin. Journal of hazardous materials 85, 165-179.

Mishra, R.K., Hubble, L.J., Martín, A., Kumar, R., Barfidokht, A., Kim, J., Musameh, M.M., Kyratzis, I.L., Wang, J., 2017. Wearable Flexible and Stretchable Glove Biosensor for On-Site Detection of Organophosphorus Chemical Threats. ACS Sensors 2, 553-561.

Mishra, R.K., Mohan, A.V., Soto, F., Chrostowski, R., Wang, J., 2017. A microneedle biosensor for minimally-invasive transdermal detection of nerve agents. Analyst 142, 918-924.

Mulchandani, A.; Chen, W.; Mulchandani, P.; Wang, J., Rogers, K. 1999. Amperometric thick-film strip electrodes for monitoring organophosphate nerve agents based on immobilized organophosphorus hydrolase. Anal. Chem. 71, 2246-2249.

Singh, V.V., 2016. Recent Advances in Electrochemical Sensors for Detecting Weapons of Mass Destruction. A Review. Electroanalysis 28, 920-935

Steiner, W.E., Klopsch, S.J., English, W.A., Clowers, B.H., Hill, H.H., 2005. Detection of a chemical warfare agent simulant in various aerosol matrixes by ion mobility time-of-flight mass spectrometry. Analytical Chemistry 77, 4792-4799.

Sylvia, J.M., Janni, J.A., Klein, J., Spencer, K.M., 2000. Surface-enhanced Raman detection of 2, 4-dinitrotoluene impurity vapor as a marker to locate landmines. Analytical chemistry 72, 5834-5840.

Wei, C., Dai, L., Roy, A., Tolle, T.B., 2006. Multifunctional chemical vapor sensors of aligned carbon nanotube and polymer composites. Journal of the American Chemical Society 128, 1412-1413.

Yang, H., Carr, P.D., McLoughlin, S.Y., Liu, J.-W., Horne, I., Qiu, X., Jeffries, C., Russell, R., Oakeshott, J.G., Ollis, D., 2003. Evolution of an organophosphate-degrading enzyme: a comparison of natural and directed evolution. Protein engineering 16, 135-145.

Yao, J., Fu, Y., Xu, W., Fan, T., Gao, Y., He, Q., Zhu, D., Cao, H., Cheng, J., 2016. Concise and Efficient Fluorescent Probe via an Intromolecular Charge Transfer for the Chemical Warfare Agent Mimic Diethylchlorophosphate Vapor Detection. Analytical chemistry 88, 2497-2501.

Zhang, W., Asiri, A.M., Liu, D., Du, D., Lin, Y., 2014. Nanomaterial-based biosensors for environmental and biological monitoring of organophosphorus pesticides and nerve agents. TrAC Trends in Analytical Chemistry 54, 1-10.

Zhu, R., Azzarelli, J.M., Swager, T.M., 2016. Wireless Hazard Badges to Detect Nerve-Agent Simulants. Angewandte Chemie 128, 9814-9818.

Table of Content (TOC)

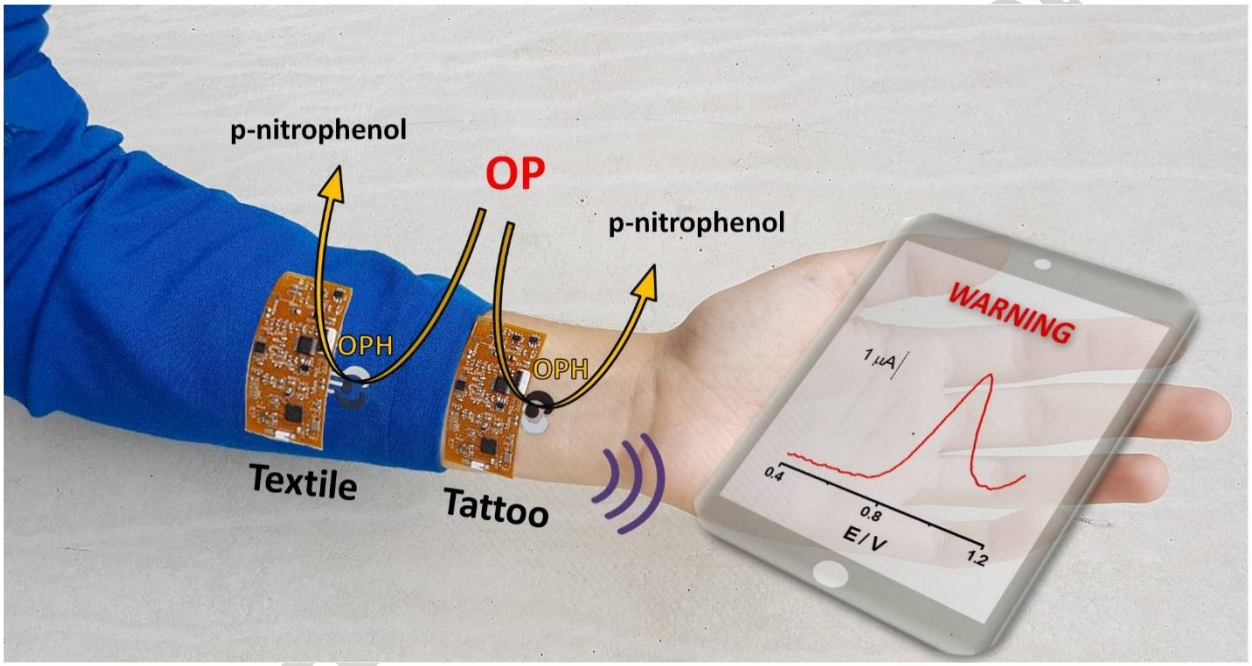

Wearable Conformable Integrated Epidermal and Textile Wireless Biosensor Systems for vapor-phase detection of nerve-agent threats

Video S1. OP spraying set-up under lab conditions.

Video S2. Epidermal tattoo sensor transference to the skin.

Video S3. Two dimensional model simulation of OP microdroplet propelled from the vapor source (left) to the electrode surface (right).

Highlights

1. Wearable epidermal Tattoo and textile biosensor for OP vapor detection
2. Simple method to nebulize OP
3. Smallest flexible square wave voltammetry-based electronic board
4. Wireless data transmission for wearable electronics